Tanzania Journal of Engineering and Technology 2024, **43**(1):46-58
OPEN ACCESS articles distributed under Creative Commons Attribution Licence [CC BY-ND]
Websites: https://ajol.org/tjet; https://tjet.udsm.ac.tz

ISSN 1821-536X (**print**); ISSN 2619-8789 (**electronic**)
https://doi.org/10.52339/tjet.v43i1.988

Regular Research Manuscript

Enhanced post deposition annealing conditions on the fabrication of high quality thermochromic vanadium dioxide films

Delvina Japhet Tarimo, Nuru Ramadhani Mlyuka† and Margaret E. Samiji*

Physics Department, University of Dar es Salaam, Box 35063, Dar es Salaam, Tanzania.
†Corresponding author email: nmlyuka@yahoo.com
*ORCID: https://orcid.org/0000-0003-2610-8290

ABSTRACT

Sputter deposition of thermochromic VO_2 thin films for smart window applications has been faced with several challenges including the need for high deposition temperature, extremely precise and narrow range of oxygen/argon flow ratio and target poisoning during sputtering. Deposition of VO_2 at room temperature without oxygen followed by post-deposition annealing has been cited as one of the potential mitigations to the challenge. In this study, the effects of post-deposition annealing conditions on the structural, electrical and optical properties of VO_2 thin films are reported. The films were prepared on soda lime glass substrates using DC magnetron sputtering of metallic vanadium target in argon atmosphere, at room temperature without oxygen followed by post-deposition annealing. The working pressure and argon flow rate were $5.2 - 5.6\,x\,10^{-3}$ mbar and 76 ml/min, respectively. Thereafter, the films were annealed in a low vacuum environment at different temperatures and times. The XRD results confirmed that all films annealed at different temperatures and times were monoclinic VO_2 except for films annealed at a temperature of 300 ^oC. The results indicate that 400 ^oC and 20 minutes are the optimum annealing temperature and time, respectively, for fabrication of high-quality VO_2 films with improved stoichiometry and crystallinity. The films had resistivity change between the semiconducting and metallic phases of one order of magnitude and the transition temperature between ~ 58 ^oC and 63 ^oC. The highest peak transmittance and best optical switching of the annealed VO_2 films was 53% and 18%, respectively, at a wavelength of 2500 nm for film thickness of 44 nm. The results suggest that room temperature deposition without oxygen followed by post-deposition annealing in a low vacuum environment may be adequate for the fabrication of switching VO_2 thin films.

ARTICLE INFO
Submitted: **Nov. 23, 2023**
Revised: **March. 13, 2024**
Accepted: **Apr, 10, 2024**
Published: **Apr., 2024**

Keywords: Thermochromism, vanadium dioxide, annealing, sputtering, surface morphology.

INTRODUCTION

Vanadium dioxide (VO2) is a phase transition metal oxide that displays reversible thermochromic property (Hou et al., 2017; Fu et al., 2006; Tsai et al., 2003). The material can change its optical and electrical properties reversibly depending on temperature (Li et al., 2015; Fang et al., 2000). The phase transition occurs at a

critical temperature (τc) of approximately 68 °C (Li et al., 2016; Granqvist et al., 2011) for bulk VO2. Below τc, VO2 has a monoclinic structure with semiconducting characteristics of high transmittance particularly in the infrared region. Above τc, VO2 has a rutile tetragonal structure with metallic characteristics of high attenuation/reflectance of electromagnetic radiation particularly in the infrared (Lyobha et al., 2018; Monfort et al., 2014). At the semiconducting-metallic transition (SMT), properties of VO2 such as electrical conductivity, structure, optical transmittance and mechanical stiffness change abruptly (Fang et al., 2000; Granqvist et al., 2010). This phase transition makes the material suitable for different applications such as smart windows, optical and electrical switching, laser protection, information storage, infrared sensors, spacecraft thermal control, and military camouflage (Hou et al., 2017; Li et al., 2016; Mlyuka, 2010; Ningyi et al., 2002).

VO2 can be prepared by different methods including; chemical vapor deposition, pulsed laser deposition, thermal evaporation, sol-gel process, and magnetron sputtering (Hou et al., 2017; Ba et al., 2016; Monfort et al., 2014; Mlyuka et al., 2009a; Kivaisi and Samiji, 1999). Each preparation method produces different and sometimes unique film structure, optical and electrical properties (Guo et al., 2021; Bukhari et al., 2020; Vostakola et al., 2017; Mlyuka and Kivaisi, 2006). Magnetron sputtering is one of the most reported techniques for VO2 fabrication because the technique mostly uses metallic vanadium targets whereby the range of the gas flow ratio between sputtering and reactive gases during sputtering varies depending on the target's composition. Specifically, the range of the oxygen/argon gas flow ratio is very narrow during deposition when metallic vanadium is used as a target (Khairy et al., 2023; Tsai et al., 2003). This is due to the existence of many oxide phases in the V-O system, meaning that even a small change in the gas flow ratio may lead to over-oxidation or reduction of the stoichiometric VO2 (Tangirala et al., 2014). Also, high deposition temperatures greater than 400 oC and precise control of the oxygen/argon ratio are required (Song et al., 2016; Kang et al., 2010; Wang et al., 2007). Furthermore, target poisoning caused by oxidation on the target surface may reduce the sputtering rate and change the stoichiometry of the deposited films when the reactive method is used (Kubart et al., 2021; Fang et al., 2000). All these make reactive deposition of VO2 from metallic vanadium targets difficult and time-consuming

Attempts have been made to fabricate VO_2 from a more stable V2O5 dielectric target through post-deposition annealing in a reducing atmosphere. On the other hand, several hindrances persist concerning the use of V2O5 targets for VO2 fabrication. These include the use of hydrogen (Corr et al., 2008), carbon monoxide (Wang *et al*., 2018), hydrogen peroxide (Wang et al., 2013) and oxalic acid (Vostakola et al., 2017) which are either explosive or toxic (MDEQ, 2024) hence requiring special safety precautions during deposition. Another attempt that has been made to fabricate VO2 is the deposition from a metallic vanadium target at room temperature followed by high-temperature annealing in a reactive gas atmosphere (Dou et al.,2015, Li et al., 2015). However, only a few studies have reported on the fabrication of VO_2 films through room temperature sputter deposition of metallic vanadium targets, followed by post-deposition annealing in a low vacuum environment (Ba et al., 2016, Li et al., 2016). Furthermore, annealing conditions for the production of high-quality VO_2 films are not well known. Improved annealing conditions may lead to the fabrication of high-quality thermochromic VO2 films. In this study, VO2 thin films were deposited on soda lime glass substrates using DC magnetron sputtering

of a metallic vanadium target at room temperature without oxygen, followed by post-deposition annealing in a low vacuum environment with residual oxygen. This method does not cause any heat damage to the magnetron in the sputter system, and has greater potential for large scale industrial production of the films (Chu et al. 2022). The effects of post-deposition annealing conditions on the structural, electrical and optical properties of the prepared films are reported.

METHODS AND MATERIALS

Experimental Details

Fabrication of VO_2 Thin Films

VO_2 thin films were deposited on soda lime glass substrates at room temperature using DC magnetron sputtering of vanadium metallic target (99.95% purity) in argon atmosphere, followed by post-deposition annealing. To obtain good adherence to the deposited films, substrates were cleaned by following standard procedures to remove organic substances, dust, and any other contaminants that were present on the surface. Before deposition, a strip on glass substrates was covered by Teflon sticky tape to create a step between the film and the substrate that can be used in the determination of film thickness. During film deposition, the base pressure was $6.5\ x\ 10^{-6}$ mbar and the working pressure was $5.2 - 5.6\ x\ 10^{-3}$ mbar, achieved after introducing argon (99.99% purity) into the deposition chamber at a flow rate of 76 ml/min. The sputtering power ranged between 100 W and 250 W while the deposition time ranged between 15 min to 40 min to achieve film thicknesses, within the range 25 nm to 180 nm, reported to possess significant optical switching (Yang *et al.*, 2019, Mlyuka *et al.*, 2009b). The films were thereafter annealed using a rapid thermal processing (RTP-1000D4) furnace at different temperatures and times. To study the effect of annealing temperature on the properties of the fabricated films, the annealing temperature was varied from 300 - 450 ^oC at a ramping rate of 60 °C/min with a fixed annealing time of 25 min. This temperature range was chosen, since it is what was reported to facilitate VO_2 growth by high temperature magnetron sputtering method (Mlyuka and Kivaisi, 2006). Furthermore, to study the effect of annealing time on the fabricated films properties, the annealing temperature was fixed at 400 ^oC and the annealing time was varied between 5 min and 25 min.

Structural and Morphological Characterization

The structure and phases of the annealed VO_2 films were investigated by X-ray diffraction (Bruker D8 Discover, XRD). The measurements were carried out using a Cu (K_α) radiation source (λ= 0.15406 nm) with a diffraction angle of 2θ; 10^o – 80^o at a scan rate of 2 ^{o}/min in a continuous scan. The XRD spectra were used to determine the degree of crystallinity of the samples and through the Scherrer formula (**Equation 1**) and measurements of the full width at half maximum ($FWHM$) of the dominant peak, crystallite sizes D were determined.

$$FWHM = \frac{k\lambda}{Dcos\theta} \quad (1)$$

where k is the shape factor of the average crystallite, in our case taken as 0.9 assuming perfect spherical grains, λ is the X-ray wavelength, and θ is the peak diffraction angle position.

The films surface morphology was investigated using a Digital Instruments Nanoscope IIIa multimode atomic force microscope. The instrument was operated in the taping mode using RTESP7, 125 µm pyramidal silicon tips with resonance frequency of ~ 300 kHz. The scan rate and scan size were 2 Hz and 2 x 2 µm, respectively. The obtained AFM images were analyzed to obtain average grain size by using the nasoscope 5.12r5 system software. Film thicknesses were

determined using the Alpha Step IQ surface profiler using 500 µm, 50 µm/s, and 50 Hz as the scan parameters presenting scan length, scan speed, and sampling rate, respectively.

Electrical Characterization

The electrical carrier concentration and mobility as well as conductivity of the samples were determined using Ecopia HMS-3000 Hall effect measurements system containing a permanent magnet source with field strength of 0.57 T. Sheet resistance of the samples in kilo-ohms per square (kΩ/□) was measured using the Jandel model RM3-AR test unit in combination with four-point probe. Electrical switching of the films was determined from sheet resistance-versus-temperature curves. A heating cell using a low-voltage DC power supply was used to heat the samples across the transition temperature. The ratio of the sheet resistance recorded at room temperature (24 ^{o}C) well below τ_c and at 100 ^{o}C (well above τ_c) was used to compute the order of electrical switching magnitude.

Optical Characterization

The Perking Elmer Spectrum BX FT-IR spectrophotometer was used to determine the optical switching of the films in the wavelength range $1800 \leq \lambda \leq 25000$ nm. This near to mid-infrared range is where VO_2 films switching is most pronounced. Measurements were taken at 25 ^{o}C (room temperature) for the semiconducting phase and 100 ^{o}C for the metallic phase of the films. Measurements at 100 ^{o}C were achieved with the aid of a heating cell consisting of a thin double plate heater in which samples were fitted. The sample temperature was monitored by pressing a thermocouple probe connected to a digital thermometer against the film surface inside the heating cell.

RESULTS AND DISCUSSION

Figure 1 displays the XRD spectra of VO_2 films annealed at different temperatures ranging from 300 ^{o}C to 450 ^{o}C. For samples annealed at 350 ^{o}C, 400 ^{o}C, and 450 ^{o}C, the spectra display a prominent diffraction peak at $2\theta \approx 14^{o}$ corresponding to (211) planes of the VO_2(B) phase as deduced from Joint Committee on Powder Diffraction Standards (JCPDS) database with card no. 01-081-2392 (Popuri *et al.,* 2013). The prominence of the (211) diffraction peak compared to other peaks reveals that the films are polycrystalline with a preferred orientation (Ji *et al.,* 2016). The spectra are also in good agreement with distinctive features of VO_2 films reported by other authors (Song *et al.,* 2016, Tsai *et al.,* 2003). At 350 ^{o}C, the composition of the films was mostly VO_2 with strong diffraction peaks corresponding to (211), (110), and (002) planes, however, extra peaks related to V_3O_5 (200) and V_4O_7 (122) phases were also observed (insert b in Figure 1). For samples annealed at 300 ^{o}C, only lower vanadium oxide phases including V_3O_5, V_4O_9, and V_4O_7 were observed (insert a in **Figure 1**) indicating insufficient oxidation of the films. This is in agreement with observations from other studies in which VO_2 samples were deposited at elevated temperatures and oxidation to VO_2 was reported to occur at deposition temperatures above 400 ^{o}C (Li *et al.,* 2016, Chu *et al.,* 2014, Guo *et al.,* 2015). **Figure 1** further shows that the intensity of the prominent (211) peak increased with increasing annealing temperature indicating an improvement in the crystallinity of the fabricated VO_2 films (Aiempanakit *et al.,* 2017, Mlyuka and Kivaisi, 2006). The average grain size was estimated by Scherrer's formula (Equation 1) and found to increase from 16 nm to 27 nm for films annealed at 400 ^{o}C and 450 ^{o}C, respectively, mostly due to increased

mobility of adatoms with increasing annealing temperature (Dou *et al.*, 2015). For higher annealing temperatures, the adatoms have enough kinetic energy to find lower energy sites before being covered by other atoms and hence better rearrangement of atoms can be realized (Ba *et al.*, 2016, Liu *et al.*, 2009). This cannot be realized at low annealing temperatures, since the condensed atoms do not have enough energy leading to poor crystallinity.

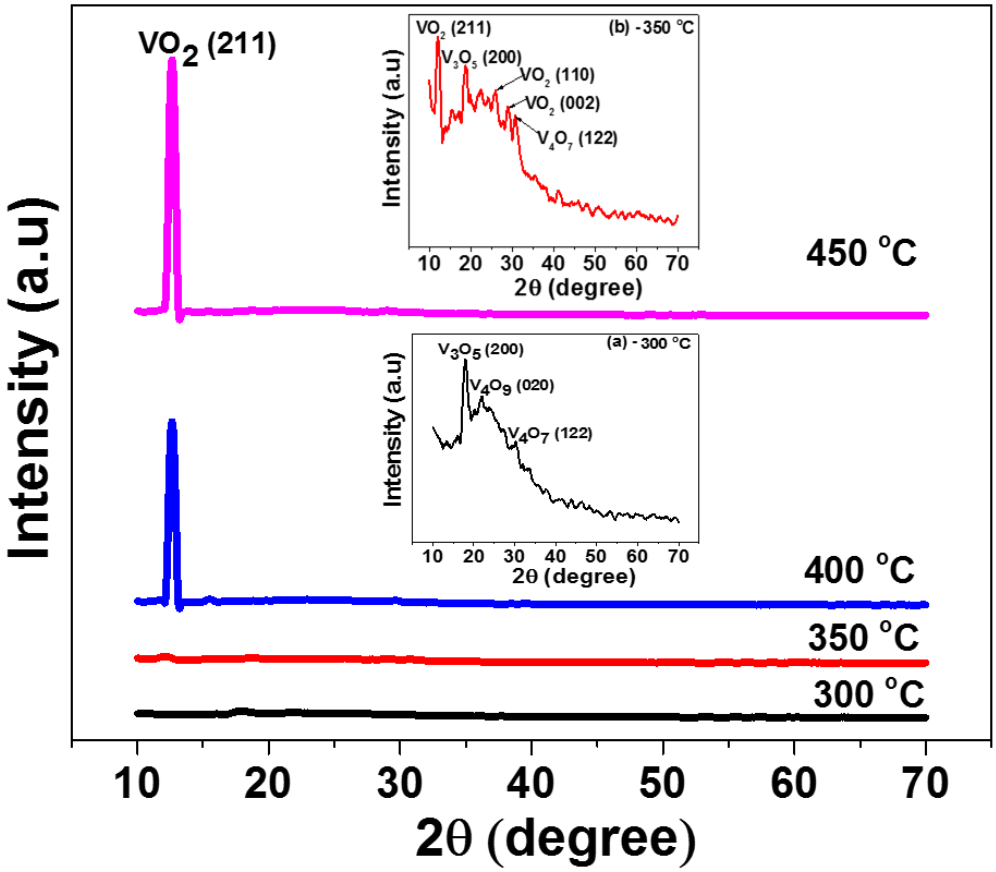

Figure 1: XRD spectra of VO_2 films annealed at 300 ºC, 350 ºC, 400 ºC, and 450 ºC. The inserts are magnified spectra for VO_2 samples annealed at 300 ºC and 350 ºC.

As for the effect of annealing time, the XRD spectra for samples annealed for 5 to 25 minutes at 400 ºC, were observed to have diffraction peaks corresponding to VO_2 (Figure 2). The figure further shows an increase in the XRD peak intensity with increasing annealing time from 5 to 20 minutes, before decreasing slightly for samples annealed for 25 minutes. This implies that an optimum annealing time is recommended for the fabrication of high-quality VO_2 films as has also been observed by other authors (Fu *et al.*, 2006, Ji *et al.*, 2016). From the XRD spectra, the average grain size of the samples determined using Scherrer's formula (Equation 1) was found to increase from 6 nm to 16 nm as the annealing time was increased from 5 to 20 minutes, thereafter, decreasing slightly to 13 nm for samples annealed for 25 minutes. Moreover, there was a slight shift of spectra peaks as the annealing time was increased. This might be attributed to increase in the lattice size and strain/compression of the samples that might have happened as a result of an increase in annealing time (Aiempanakit *et al.*, 2017, Tselev *et al.*,2010).

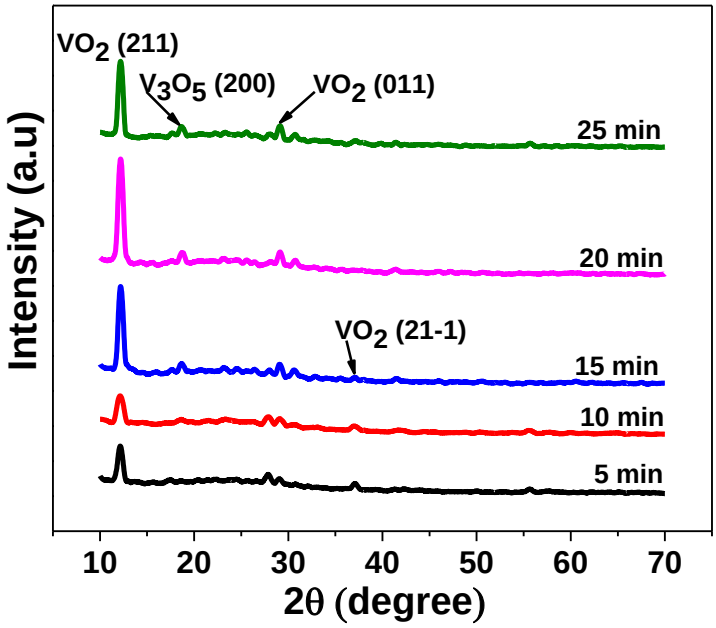

Figure 2: XRD spectra of VO_2 films annealed for 5, 10, 15, 20 and 25 minutes.

Figure 3 (a) shows the AFM image of the as-deposited VO_2 films whereby the surface morphology was found to be uniform and densely packed with an average grain size of 161 nm^2 as determined by Nanoscope 5.12r5 system software. Figure 3 (b, c, and d) displays images of VO_2 films annealed at temperatures of 300 ºC, 350 ºC, and 450 ºC, respectively. From the figures, it is evident that the films' morphologies evolve with an increase in annealing temperature whereby films annealed at 300 ºC and 350 ºC showed well-developed elongated grains whereas those annealed at 450 °C had very large grains that seemed to have coalesced into a more continuous film. The average grain size of the films increased with an increase in annealing temperature at 374 nm^2, 643 nm^2, and 1107 nm^2 for films annealed at 300 ºC, 350 ºC, and 450 °C, respectively as presented in **Figure 3 (e)**. The increase in average grain size with an increase in annealing temperature is due to enhanced atom mobility and/hence migration across grain boundaries and recrystallization at higher temperatures leading to the formation of larger grains as suggested by Thorntons film growth model (Thornton, 1986). The evolution of the films microstructure with an increase in annealing temperature is evident from these results, however, the optimum annealing temperature is recommended to obtain high-quality VO_2 films (Corr *et al.*, 2008, Wang *et al.*, 2007).

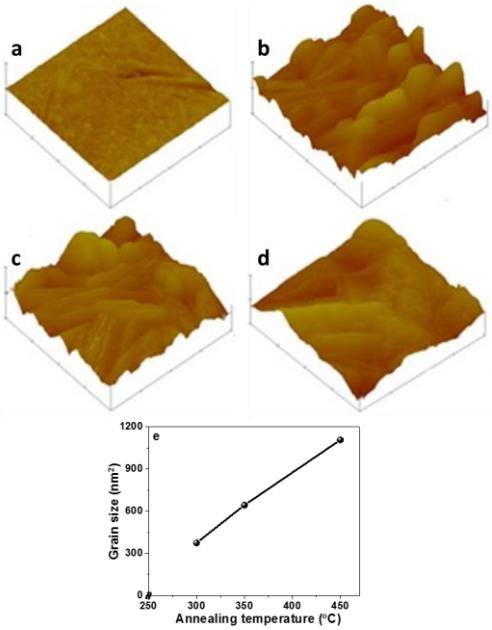

Figure 3: (a and b, c, d) AFM images for VO_2 films (a) as-deposited, and annealed at; (b) 300 ºC, (c) 350 ºC, and (d) 450 ºC, respectively, and (e) grain size dependence on annealing temperature (the lines are for guiding the eye).

Figure 4 (a - d) shows AFM images of VO_2 films annealed at different time intervals at 400 °C substrate temperature. Films annealed for 5 min exhibited a compact surface with many small grains of 290 nm^2 in size (Figure 4 (a)). At 10 min annealing time, the films appear rougher, with a relatively larger grain of 368 nm^2 in size (Figure 4 (b)). At 15 min annealing time, the grains roughness appears to decrease slightly, and grain size increases further to 416 nm^2 (Figure. 4 (c)). At 20 min annealing time, the average grain size increased further to 548 nm^2 and appears more uniform across the image (Figure 4 (d)).

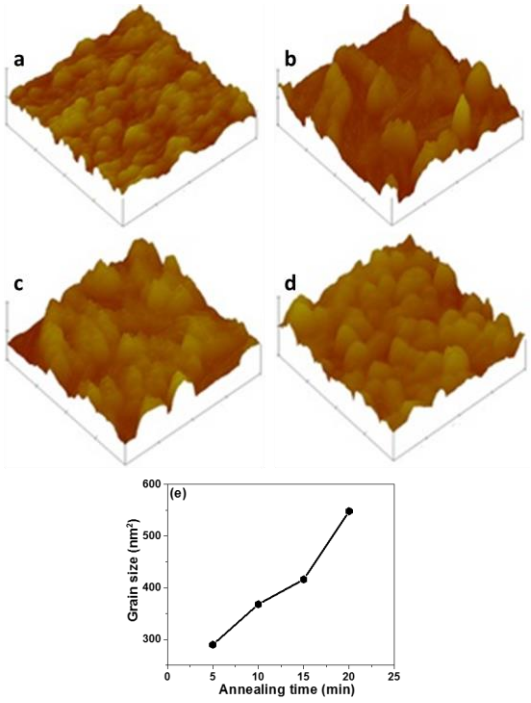

Figure 4: (a and b, c, d) AFM image of VO_2 films annealed for (a) 5 min, (b) 10 min, (c) 15 min, and (d) 20 min, respectively, and (e) grain size dependence on annealing time (the lines are for guiding the eye).

Sheet resistance as a function of the annealing temperature of VO_2 films is shown in Figure 5 (a – d). During measurements, the temperature of the sample was increased from 25 ^oC to 100 ^oC followed by subsequent cooling back to 25 ^oC. The best annealed VO_2 samples had a resistivity change between the semiconducting to metallic phases of one order of magnitude in agreement with results reported for high-temperature deposited VO_2 films (Mussa *et al.*, 2018, Dou *et al.*,2015, Guo *et al.*, 2014). The sheet resistance switching however was not very sharp due to the size of the grains as has been observed before (Xu *et al.*, 2012). This made a determination of τ_c to be challenging, however, taking the value of τ_c as a midpoint between heating and cooling curves of temperature-dependent sheet resistance, the τ_c was estimated to be between ~ 58 ^oC to 63 ^oC consistent with the values reported for VO_2 thin films deposited under high-temperature reactive sputtering (Haji *et al.*,2023, Li *et al.*, 2016, Mlyuka *et al.*, 2009b).

Conductivity and carrier concentration of the films as determined by the Hall Effect measurements system, were found to decrease while charge carrier mobility increased with an increase in annealing temperature as shown in Figure 6 (a and b). The highest values of electrical conductivity and carrier concentration were 15.7 $(\Omega cm)^{-1}$ and 2.4 $x\ 10^{20}$ cm^{-3}, respectively obtained for VO_2 films annealed at 300 ^oC. At higher annealing temperatures, conductivity and carrier concentration decreased to below 2 $(\Omega cm)^{-1}$ and between $0.4\,x10^{19}$ and $2.1x10^{19}$, respectively. The corresponding values of resistivity are just the reciprocal of conductivity and are shown in Figure 6 (d). Carrier mobility on the other hand slightly increased with increasing annealing temperature as depicted in Figure 6 (c). The decrease in carrier concentration and conductivity is due to an increase in oxidation of the films into a semiconducting VO_2 as the annealing temperature was increased (Tsai *et al.*, 2003). On the other hand, increased carrier mobility with an increase in annealing temperature is a result of improved crystallinity of the films as was observed from XRD data, making the flow of charge

carries easier. An increase in mobility of carriers is expected to increase conductivity, however, in this study this was coupled with a decrease in carrier concentration, resulting in an overall decrease in conductivity.

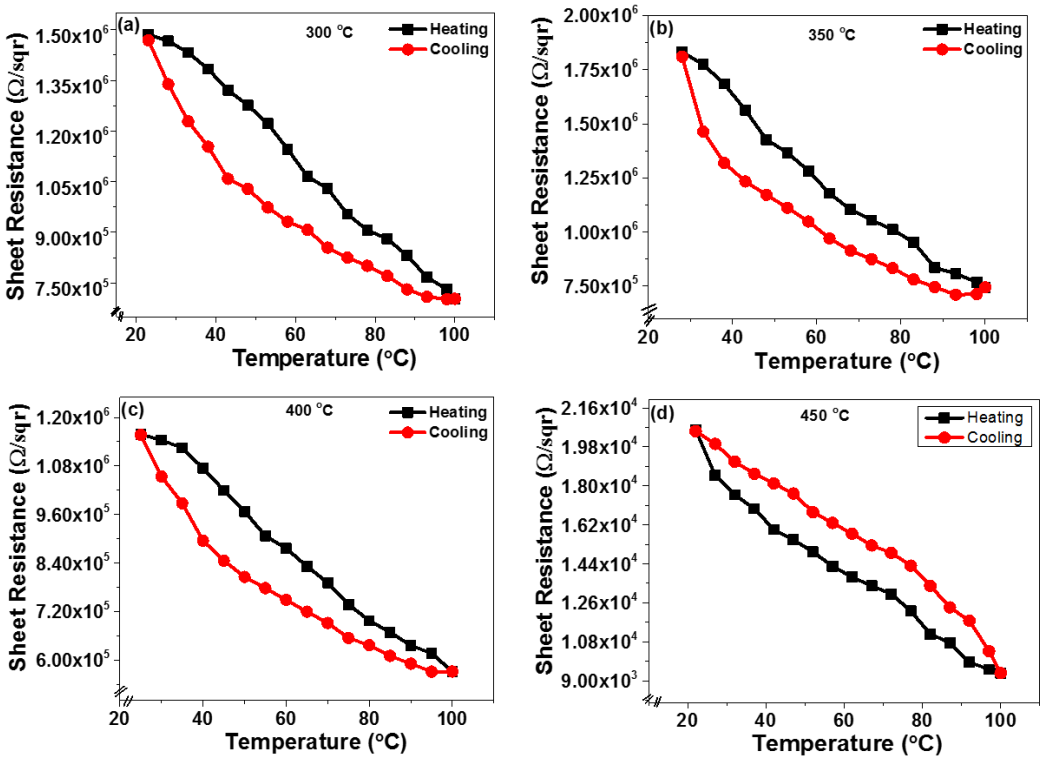

Figure 5: Sheet Resistance versus temperature curves for films annealed at (a) 300 ºC, (b) 350 ºC, (c) 400 ºC and (d) 450 ºC, respectively.

Figure 7 (a-c) displays the spectral transmittance of annealed VO_2 films in both semiconducting and metallic phases in the wavelength range of $1800 \leq \lambda \leq 6000$ nm. Optical transmittance of VO_2 thin films strongly depends on film thickness and hence we present values for thicknesses reported to achieve significant optical switching (Yang *et al.*, 2019). Films with a thickness of 44 nm showed the best optical transmittance switching of about 18%, from 53% for the semiconducting phase at 25 °C to 12% for the metallic phase at 100 ºC obtained at $\lambda = 2500$ nm, a wavelength at which VO_2 displays maximum switching amplitude (Liu *et al.*, 2009, Luo *et al.*, 2016). As the film thickness increased to 113 nm, the transmittance switching amplitude decreased to 18% as shown in the figure. The peak transmittance in the semiconducting phase also decreased with an increase in film thickness, from 53% at $\lambda =$ 2500 nm for 44 nm thin films to 18% for 113 nm thin films. The optical data suggests that room temperature deposition without oxygen followed by post-deposition annealing in a low vacuum environment may be adequate for the fabrication of switching VO_2 thin films.

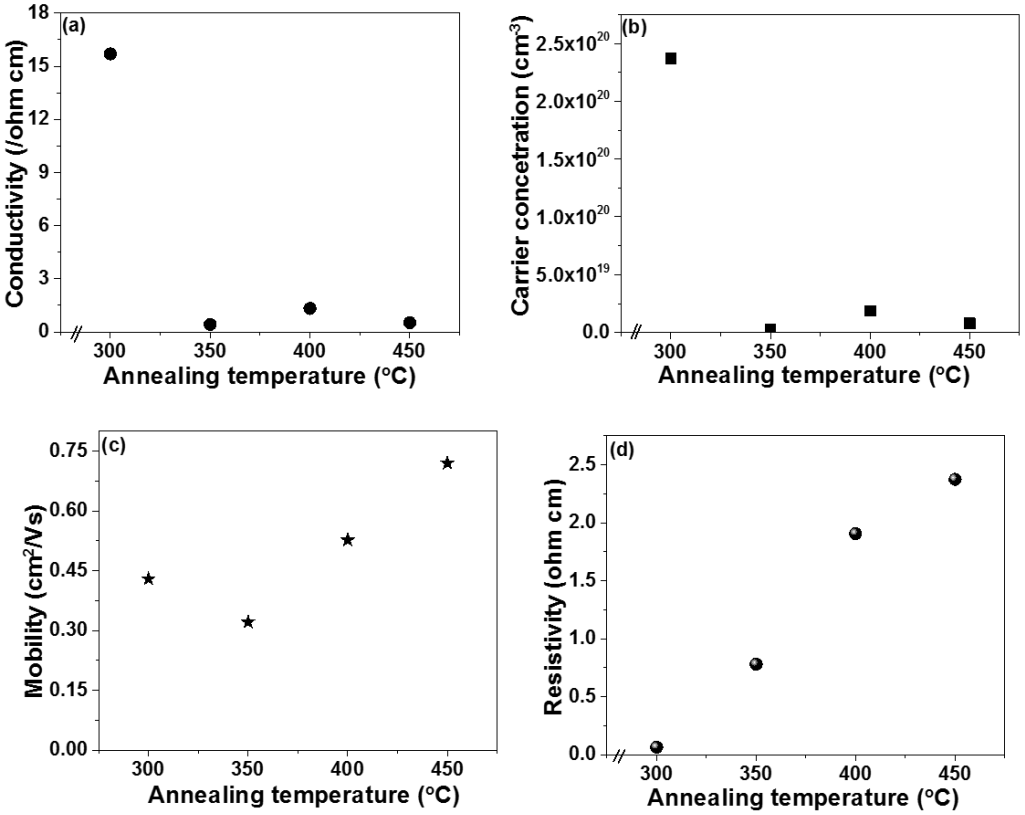

Figure 6: The variation of (a) conductivity, (b) carrier concentration, (c) mobility, and (d) resistivity of VO_2 films with annealing temperature.

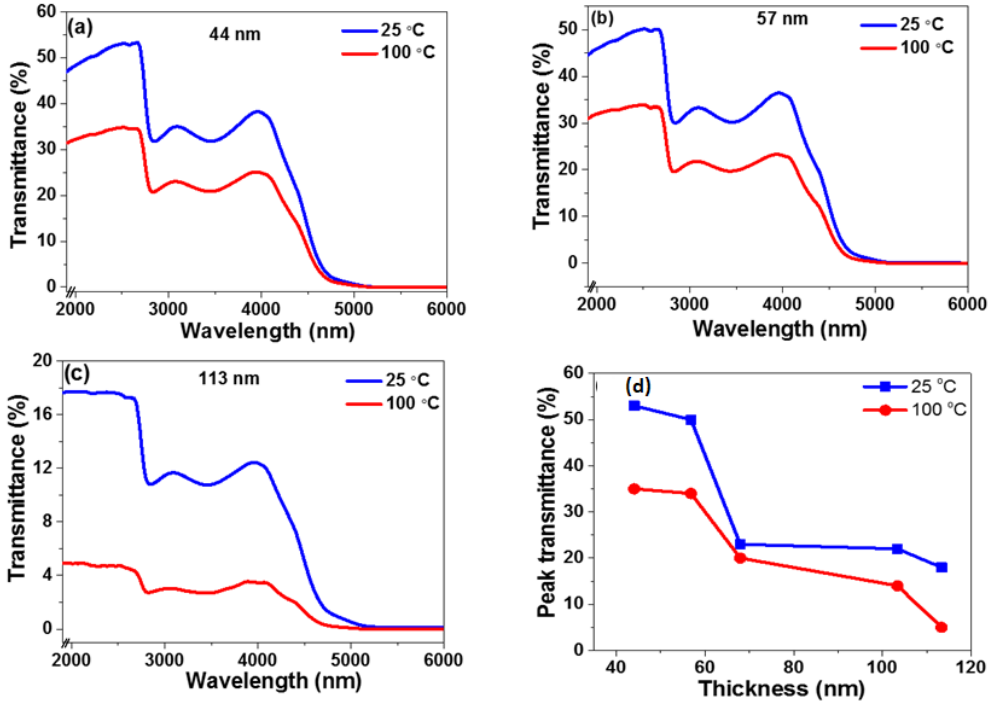

Figure 7: (a-c) Low and high-temperature spectral transmittance of thermochromic VO_2 films with different thicknesses, annealed at 400 ºC. (d) Switching magnitude of VO_2 as a function of film thickness (the lines are meant to guide the eye).

CONCLUSION

In this study, the effects of post-deposition annealing temperature and time on the properties of VO_2 films deposited using DC magnetron sputtering at room temperature without oxygen followed by post-deposition annealing in a low vacuum environment were investigated. The XRD results confirmed that all films annealed at different temperatures and times were monoclinic VO_2 except for films annealed at 300 ^oC. It was found that 400 ^oC and 20 minutes are the optimum annealing temperature and time for the fabrication of high-quality VO_2 films with improved stoichiometry and crystallinity in a low vacuum environment. Resistivity switching of the films between the semiconducting and metallic phases was of one order of magnitude and the transition temperature was determined to be between ~58 ^oC to 63 ^oC consistent with the values reported for high-temperature deposition of VO_2 thin films. As the films thickness was increased, the overall optical transmittance decreased, that is, films with a thickness of 44 nm and annealed at 400 ^oC showed the best optical switching of about 18%, from 53% for the semiconducting phase of VO_2 at room temperature to 12% for the metallic phase of VO_2 at 100 ^oC evaluated at a wavelength, λ = 2500 nm. These results demonstrate that DC magnetron sputtering at room temperature without oxygen followed by post-deposition annealing is a viable alternative process to be followed for the fabrication of high-quality VO_2 thin films.

ACKNOWLEDGEMENTS

The authors acknowledge the International Science Programme (ISP) and the University of Dar es Salaam for laboratory facilities and research materials. Prof. Tsong P. Perng and Dr. Ming-Wei Liao of National Tsing Hua University, Taiwan are very much appreciated for XRD analysis. DJT is grateful for partial financial support from ISP.

REFERENCES

Aiempanakit M., Kosum J. and Kaewphong T. (2017). The Influence of Post Annealing on the Structure and Optical Properties of Vanadium Oxide Thin Films, Mater. Today Proc., 4(5): 6015-21. https://doi.org/10.1016/j.matpr.2017.06.088

Ba C.O.F., Fortin V., Bah S.T., Vallée R. and Pandurang A. (2016). Formation of VO_2 by Rapid Thermal Annealing and Cooling of Sputtered Vanadium Thin Films, J. Vac. Sci. Technol. A, 34(3): 031505. https://doi.org/10.1116/1.4944606

Bukhari S.A., Kumar S., Kumar P., Gumfekar S.P., Chung H-J., Thundat T. and Goswami A. (2020). The effect of oxygen flow rate on metal-insulator transition (MIT) characteristics of vanadium dioxide (VO_2) thin films by pulsed laser deposition (PLD), Appl. Surf. Sci., 529: 146995. https://doi.org/10.1016/j.apsusc.2020.146995

Chu X., Xie Q., Zhang X., Guo B., Liao J. and Zhao X. (2022). Fabrication and Optical Characterization of VO_2-Based Thin Films Deposited on Practical Float Glass by Magnetron Sputtering and Professional Annealing, Materials (Basel), 15(9):2990. https://doi.org/10.3390/ma15092990

Chu X., Tao H., Wan M., Wang S., Ning Z., Xu N. and Zhao X. (2014). Effect of Annealing Duration and Substrates on Structure and Property of Vanadium Dioxide Films, J. Wuhan Univ. Technol. Mater. Sci. Ed., 29: 1117-23. https://doi.org/10.1007/s11595-014-1052-y

Corr S.A., Grossman M., Furman J.D., Melot B.C., Cheetham A.K., Heier K.R. and Seshadri R. (2008). Controlled Reduction of Vanadium Oxide Nanoscrolls: Crystal Structure, Morphology, and Electrical

Properties, Chem. Mater., 20(20): 6396-404. https://doi.org/10.1021/cm801539f

Dou Y.K., Li J.B., Cao M.S., Su D.Z., Rehman F., Zhang J.S. and Jin H.B. (2015). Oxidizing Annealing Effects on VO_2 Films with Different Microstructures, Appl. Surf. Sci., 345: 232-7. https://doi.org/10.1016/j.apsusc.2015.03.044

Fang G.J., Liu Z.L., Wang Y.Q., Liu H.H., and Yao K.L. (2000). Orientated growth of V_2O_5 Electrochromic Thin Films on Transparent Conductive Glass by Pulsed Excimer Laser Ablation Technique, J Phys D Appl Phys., 33(23): 3018. 10.1088/0022-3727/33/23/302

Fu G., Polity A., Volbers N. and Meyer B.K. (2006). Annealing effects on VO_2 thin films deposited by reactive sputtering, Thin Solid Films, 515(4): 2519-22. https://doi.org/10.1016/j.tsf.2006.04.025

Granqvist C.G., Green S.V., Li S.Y., Mlyuka N.R., Niklasson G.A. and Avendaño E. (2011). Advances in Electrochromics and Thermochromics: Applications to Sustainable Energy. In: Advances in Nanotechnology, 8: 449-460, Nova Science Publishers, Inc. Hauppauge, New York.

Granqvist C.G., Green S.V., Li S.Y., Mlyuka N.R., Niklasson G.A. and Avendaño E. (2010). Chromogenics for Sustainable Energy: Some Advances in Thermochromics and Electrochromics, Advances in Science and Technology, 75: 55-64. https://doi.org/10.4028/www.scientific.net/AST.75.55

Guo X., Tan Y., Hu Y., Zafar Z., Liu J. and Zou J. (2021). High quality VO_2 thin films synthesized from V_2O_5 powder for sensitive near-infrared detection, Sci. Rep., 11(1): 21749. https://doi.org/10.1038/s41598-021-01025-8

Guo Y., Xu H., Zou C., Yang Z., Tong B., Yu J., Zhang Y., Zhao L. and Wang Y. (2015). Evolution of Structure and Electrical Properties with Annealing Time in Solution-Based VO_2 Thin Films, J. Alloys Compd., 622: 913-7. https://doi.org/10.1016/j.jallcom.2014.11.027

Haji H.F., Numan N., Madiba I.G., Mabakachaba B., Mtshali C., Khumalo Z., Kotsedi L., Mlyuka N., Samiji M. and Maaza M. (2023). Zn and W Co-doped VO_2-Based Thin Films Prepared by DC Magnetron Sputtering: Improved Luminous Transmittance and Reduced Transition Temperature. J. Electron. Mater., 52(6): 4020-4029. https://doi.org/10.1007/s11664-023-10382-1

Hou D., Lu Y. and Song F. (2017). Effects of Substrate Temperature on Properties of Vanadium Oxide Thin Films on Si Substrate, Proc. Second Int Conf Photonics Opt Eng., 10256:102560R. https://doi.org/10.1117/12.2256432

Ji C., Wu Z., Wu X., Feng H., Ma X. and Jiang Y. (2016). Effects of Annealing Time on the Application of Vanadium Dioxide Films in Smart Windows. Proc. 8th Int. Symp. Adv. Opt. Manuf. Test Technol. Optoelectron Mater Devices, 9686: 12. https://doi.org/10.1117/12.2242821

Khairy K.T., Song Y., Yoon J.H., Montero J., Österlund L., Kim S. and Song P. (2023). Thermochromic properties of vanadium oxide thin films prepared by reactive magnetron sputtering at different oxygen concentrations, Vacuum, 210: 111887. https://doi.org/10.1016/j.vacuum.2023.111887

Kang L., Gao Y., Zhang Z., Du J., Cao C., Chen Z. and Luo H. (2010). Effects of Annealing Parameters on Optical Properties of Thermochromic VO_2 Films Prepared in Aqueous Solution, J. Phys. Chem. C., 114(4): 1901-11. https://doi.org/10.1021/jp909009w

Kivaisi R.T. and Samiji M. (1999). Optical and Electrical Properties of Vanadium Dioxide Films Prepared under Optimized RF Sputtering

Conditions, Sol. Energy Mater. Sol. Cells, 57(2): 141-52. https://doi.org/10.1016/S0927-0248(98)00166-4

Kubart T., Fernandes D.F. and Nyberg T. (2021). On the Description of Metal Ion Return in Reactive High-Power Impulse Magnetron Sputtering, Surf. Coat. Technol., 418: 127234 (1-5). https://doi.org/10.1016/j.surfcoat.2021.127234

Li D., Huang W., Song L. and Shi Q. (2015). Thermal Stability of VO_2 Thin Films Deposited by sol–gel Method, J Sol-Gel Sci Technol., 75: 189-97. https://doi.org/10.1007/s10971-015-3688-2

Li Y., Wang D., Liu J., Ren L., Liu Y. and Zou K. (2016). Effect of Annealing Temperature on the Structure and Properties of Vanadium Oxide Films, Opt. Mater. Express., 6(5): 1552. https://doi.org/10.1364/OME.6.001552

Liu D.Q., Zheng W.W., Cheng H.F. and Liu H.T. (2009). Thermochromic VO_2 Thin Film Prepared by Post Annealing Treatment of V_2O_5 Thin Film, Adv. Mater. Res., 79–82: 747-50. https://doi.org/10.4028/www.scientific.net/AMR.79-82.747

Luo Y.Y., Pan S.S., Xu S.C., Zhong L., Wang H. and Li G.H. (2016). Influence of Sputtering Power on the Phase Transition Performance of VO_2 Thin Films Grown by Magnetron Sputtering, J. Alloys Compd., 664: 626-31. https://doi.org/10.1016/j.jallcom.2015.12.222

Lyobha C.J., Mlyuka N.R. and Samiji M.E. (2018). Effects of Aluminium and Tungsten Co-doping on the Optical Properties of VO_2 Based Thin Films, Tanz. J. Sci., 44 (4): 91-99.

MDEQ (Montana Department of Environmental Quality). Chemical_Inventory_Sheet. Available online at https://deq.mt.gov/files/Land/Hazwaste/Documents/Chemical_Inventory_Sheet.xls. Retrieved on 30th April 2024.

Mlyuka N.R. (2010) Vanadium Dioxide Based Thin Films: Enhanced Performance for Smart Window Applications. PhD Thesis, University of Dar es Salaam.

Mlyuka N.R. and Kivaisi R.T. (2006). Correlation Between Optical, Electrical and Structural Properties of Vanadium Dioxide Thin Films, J. Mater. Sci., 41(17): 5619-24. https://doi.org/10.1007/s10853-006-0261-y

Mlyuka N. R., Niklasson G.A. and Granqvist C.G. (2009a). Mg Doping of Thermochromic VO_2 Films Enhances the Optical Transmittance and Decreases the Metal-Insulator Transition Temperature, Appl. Phys. Lett, 95(17): 1-4. https://doi.org/10.1063/1.3229949

Mlyuka N.R., Niklasson G.A. and Granqvist C.G. (2009b). Thermochromic Multilayer Films of VO_2 and TiO_2 with Enhanced Transmittance, Sol. Energy Mater. Sol. Cells, 93(9): 1685-1687. https://doi.org/10.1016/j.solmat.2009.03.021

Monfort O., Roch T., Satrapinskyy L., Gregor M., Plecenik T., Plecenik A. and Plesch G. (2014). Reduction of V_2O_5 Thin Films Deposited by Aqueous Sol-Gel Method to VO_2 (B) and Investigation of its Photocatalytic Activity, Appl. Surf. Sci., 322: 21-7. https://doi.org/10.1016/j.apsusc.2014.10.009

Mussa M., Mlyuka N.R. and Samiji M.E. (2018). Hall Effect Parameters of Aluminium and Tungsten Co-Doped VO_2 Thin Films. Tanz. J. Sci., 44 (4): 100-105.

Ningyi Y., Jinhua L. and Chenglu L. (2002). Valence Reduction Process from Sol-Gel V_2O_5 to VO_2 Thin Films, Appl. Surf. Sci., 191: 176-80. https://doi.org/10.1016/S0169-4332(02)00180-0

Popuri S.R., Miclau M., Artemenko A., Labrugere C., Villesuzanne A. and Pollet M. (2013). Rapid

Hydrothermal Synthesis of VO_2 (B) and its Conversion to Thermochromic VO_2 (M1). Inorg. Chem., 52(9): 4780-5. https://doi.org/10.1021/ic301201k

Song F. and White B.E. (2016). Growth of Ultra-Thin Vanadium Dioxide Thin Films using Magnetron Sputtering.;1–11. Available online at https://arxiv.org/pdf/1608.03911.pdf . Retrieved on 5th November 2023.

Tangirala M., Zhang K., Nminibapiel D., Pallem V., Dussarrat C., Cao W., Adam T.N., Johnson C.S., Elsayed-Ali H.E. and Baumgart H. (2014). Physical Analysis of VO_2 Films Grown by Atomic Layer Deposition and RF Magnetron Sputtering, ECS J. Solid State Sci. Technol., 3(6): N89-N94. 10.1149/2.006406jss

Thornton J. A. (1986). The Microstructure of Sputter Deposited Coatings. J. Vac. Sci. Technol., 4(6): 359-365. https://doi.org/10.1116/1.573628

Tsai K-Y., Chin T-S. and Shieh H-PD. (2003). Properties of VO_2 Films Sputter-Deposited from V_2O_5 Target, Jpn J Appl Phys., 42(7R): 4480-3. 10.1143/JJAP.42.4480

Tselev A., Meunier V., Strelcov E., Shelton W.A., Luk'yanchuk I.A., Jones K., Proksch R., Kolmakov A. and Kalinin S.V. (2010). Mesoscopic Metal-Insulator Transition at Ferroelastic Domain Walls in VO_2, ACS Nano, 4(8): 4412-9. https://doi.org/10.1021/nn1004364

Vostakola M.F., Yekta B.E. and Mirkazemi S.M. (2017). The Effects of Vanadium Pentoxide to Oxalic Acid Ratio and Different Atmospheres on the Formation of VO_2 Nanopowders Synthesized via Sol-Gel Method, J. Electron. Mater., 46(11): 6689-97. https://doi.org/10.1007/s11664-017-5712-5

Wang N., Magdassi S., Mandler D. and Long Y. (2013). Simple Sol-Gel Process and One-Step Annealing of Vanadium Dioxide Thin Films: Synthesis and Thermochromic Properties, Thin Solid Films, 534: 594-8. https://doi.org/10.1016/j.tsf.2013.01.074

Wang S., Owusu K.A., Mai L., Ke Y., Zhou Y., Hu P., Magdassi S. and Long Y. (2018). Vanadium Dioxide for Energy Conservation and Energy Storage Applications: Synthesis and Performance Improvement, Appl. Energy, 211: 200-17. https://doi.org/10.1016/j.apenergy.2017.11.039

Wang Y.L., Li M.C. and Zhao L.C. (2007). The Effects of Vacuum Annealing on the Structure of VO_2 Thin Films, Surf. Coat. Technol., 201(15): 6772-6. 10.1088/1742-6596/2431/1/012055

Xu X., He X., Wang H., Gu Q., Shi S., Xing H., Wang C., Zhang J., Chen X. and Chu J. (2012). The Extremely Narrow Hysteresis Width of Phase Transition in Nanocrystalline VO_2 Thin Films with the Flake Grain Structures, Appl. Surf. Sci., 261: 83-7. https://doi.org/10.1016/j.apsusc.2012.07.098

Yang Y., Cao X., Sun G., Long S., Chang T., Li X. and Jin P. (2019). Transmittance Change with Thickness for Polycrystalline VO_2 Films Deposited at Room Temperature, J. Alloys Compd., 791(30): 648-654. https://doi.org/10.1016/j.jallcom.2019.03.278